

Magnetic field mediated low-temperature resistivity upturn in electron-doped $\text{La}_{1-x}\text{Hf}_x\text{MnO}_3$ manganite oxides

E. J. Guo,^{1,2,a)} L. Wang,¹ Z. P. Wu,¹ L. Wang,² H. B. Lu,² K. J. Jin,² and J. Gao^{1,b)}

¹Department of Physics, The University of Hong Kong, Pokfulam Road, Hong Kong

²Beijing National Laboratory for Condensed Matter Physics, Institute of Physics, Chinese Academy of Sciences, Beijing 100190, China

(Received 11 September 2012; accepted 19 November 2012; published online 20 December 2012)

The low-temperature transport properties were systematically studied on the electron-doped polycrystalline $\text{La}_{1-x}\text{Hf}_x\text{MnO}_3$ ($x=0.2$ and 0.3) compounds at the presence of external magnetic fields. The resistivity of all samples exhibits a generally low-temperature resistance upturn behavior under zero magnetic field at the temperature of T_{\min} , which first shifts towards lower temperature at low magnetic field ($H < 0.75$ T) and then moves back to higher temperature as magnetic fields increase, which is greatly different with the previous results on the hole-doped manganites. The best fitting of low-temperature resistivity could be made by considering both electron-electron ($e-e$) interactions in terms of $T^{1/2}$ dependence and Kondo-like spin dependent scattering in terms of $\ln T$ dependence at all magnetic fields. Our results will be meaningful to understand the underlying physical mechanism of low-temperature resistivity minimum behavior in the electron-doped manganites. © 2012 American Institute of Physics. [<http://dx.doi.org/10.1063/1.4770320>]

I. INTRODUCTION

In the doped manganites, the interactions among the charge, orbital, spin, and lattice will result in a variety of intriguing phenomenon, such as the colossal magnetoresistance (CMR),^{1,2} charge-orbital-ordering (COO),^{3,4} multiferroelectric,⁵ and high- T_c superconductivity.^{6,7} During the years, much attention has been focused on the electric and magnetic transport properties of doped manganites at low temperature.⁸⁻¹⁴ With temperature decrease, the contribution from the electron-phonon interaction will be greatly weakened and the Coulomb interaction cannot be ignored as usual. Thus, the low-temperature transport behavior may reflect their intrinsic mechanism. Several works have provided evidence for the existence of the resistivity minimum at low temperature in the doped manganites, no matter the polycrystalline, single crystals, or the epitaxial thin films. The observed phenomenon is similar to the Kondo effect, which was first found in the crystalline noble-metal alloys with low magnetic impurity concentration. They attributed it to the exchange interaction between itinerant conduction electrons and localized spin impurities. However, the difference between Kondo effect and the effects observed on the manganites is that the temperature for resistivity minima of Kondo effect, T_{\min} , is independent on the applied magnetic fields. Rozenberg *et al.*⁸ obtained a shallow minimum on ceramic $\text{La}_{0.5}\text{Pb}_{0.5}\text{MnO}_3$ sample at temperature of 25–30 K under zero magnetic field. The T_{\min} shifts towards lower temperatures under external magnetic fields and disappears at a certain field. Xu *et al.*⁹ found the similar variation trend of T_{\min} on polycrystalline $\text{La}_{2/3}\text{Ca}_{1/3}\text{MnO}_3$ under various magnetic fields. However,

they declared that such behavior not only disappeared but also almost independent when the magnetic field is higher than 1 T. Kumar *et al.* reported the observation of low-temperature resistivity minima in $\text{La}_{0.7}\text{Ca}_{0.3}\text{MnO}_3$ thin films and found that T_{\min} moves first to the higher temperature at low magnetic fields and then to lower temperature at high magnetic field.¹⁰ It was obvious that different effects of magnetic fields on the low-temperature upturn for polycrystalline samples and thin films were attributed to different electronic conduction mechanisms. So far, in order to explain this interesting and abnormal behavior at low temperature, several models have been proposed, such as spin-polarized tunneling through the grain boundaries, Kondo-type effect due to the spin disorder, and quantum corrections to conductivity (QCC) effect including electron-electron ($e-e$) interactions, and weak localization effects due to the finite dimensions of systems.⁸⁻¹⁴ It is widely accepted that the model of intergrain spin-polarized tunneling through grain boundaries (GBs) may account for resistivity minimum behaviors in the polycrystalline.⁸ However, the QCC effects may be the dominant mechanism in manganite single crystals and thin films, which was proven both experimentally and theoretically.¹⁰ Although much effort had been devoted to explain the resistivity minimum behavior in manganites, but up to date, clear conclusions have not been drawn since too many different experiment results and different interpretations existed.

For many years, some researchers attempt to substitute tetravalent ions like Ce^{4+} , Te^{4+} , Sn^{4+} , Sb^{4+} , and Pb^{4+} at the La site in order to gain electron-doped manganites.^{8,15-21} It is generally believed that the electron-doped manganites exhibit CMR effect via the double exchange (DE) between the Mn^{3+} - Mn^{2+} ions, instead of DE between Mn^{3+} - Mn^{4+} ions in hole-doped compounds. This stimulates the hopes of manufacturing all manganites p - n junctions and spintronic devices in the near future. Unlike the other tetravalent elements, Hf typically

^{a)}Present address: IFW-Dresden, 01069 Dresden, Germany. Email: ejguophysics@gmail.com.

^{b)}Author to whom correspondence should be addressed. Electronic mail: jugao@hku.hk.

shows a single tetravalent or zero valence states. This makes it relatively simple and reliable to study the electronic structure of $\text{La}_{1-x}\text{Hf}_x\text{MnO}_3$ system. Our previous results from the x-ray photoemission spectroscopy (XPS) and magnetically Hall measurement prove that the $\text{La}_{1-x}\text{Hf}_x\text{MnO}_3$ system is a typical electron-doped manganite.^{22–24} However, as far as we know, the low-temperature transport property of electron-doped manganites is limited, and no attempt was done on Hf-doped manganites. In this paper, the effects of applied magnetic field on the low-temperature transport property of polycrystalline $\text{La}_{1-x}\text{Hf}_x\text{MnO}_3$ (LHMO) compounds with Hf doping levels of 0.2 and 0.3 were studied. The results show that the low-temperature resistivity minimum behavior is strongly dependent on the applied magnetic field. The variation trend of T_{\min} in our case is not consistent with the previous works like Refs. 8–10, but T_{\min} shifts to lower temperature at low field region and then moves to higher temperature at high field region. We found that two possible mechanisms of e - e interaction and spin dependent scattering coexistence under various magnetic fields might be responsible for such behavior.

II. EXPERIMENT DETAILS

The LHMO bulk polycrystalline samples with different doping levels $x=0.2$ and 0.3 were prepared by standard solid-state reaction method. Stoichiometric amounts of La_2O_3 , HfO_2 , and MnO_2 high-purity powders were mixed together sufficiently and preheated to 900°C for 12 h. Then, it was pressed into pellet and sintered in air at 1200°C for 96 h with intermediate grindings and cooled down to room temperature slowly. A second sintering by repeating the second step was carried out in order to improve the purity of samples. The structure of LHMO samples was examined by powder

x-ray diffraction (XRD) measurements using Cu $K\alpha$ radiation (the results were shown and discussed in detail in Ref. 24). The electrical transport properties (ρ - T) were measured by standard four-probe method using physical property measurement system (PPMS, Quantum Design) in the temperature range of 5–300 K and the magnetic field range of 0–5 T. Before applying the next fields, the samples were warmed up to the room temperature and kept for 10 min. Then, the resistances of samples were recorded during the cooling down process. The electric contacts were made using silver paste with the contacting resistance below $0.05\ \Omega$ at room temperature. All the ρ - T curves were measured through field cooling process.

III. RESULTS AND DISCUSSIONS

As shown in Fig. 1, the temperature dependence of resistivity (ρ) and magnetoresistance (MR = $[\text{R}(H) - \text{R}(0)] \times 100\% / \text{R}(0)$) for LHMO(0.2) and LHMO(0.3) was measured under various magnetic fields. Both of them present a metal-to-insulator transition (MIT) with decrease in temperature. The resistivity of LHMO(0.3) is smaller than that of LHMO(0.2) due to the high doping level induced increase of carrier density. For LHMO(0.2), two independent peaks are found, one is a sharp peak at $\sim 232\ \text{K}$ and another is a broad peak at $\sim 210\ \text{K}$ (shown in Fig. 1(a)). The results on the temperature dependent magnetization for LHMO(0.2) show a paramagnetic-to-ferromagnetic transition at $\sim 230\ \text{K}$, confirming that the MIT happens at the temperature of first sharp peak.²⁴ As shown in Fig. 1(b), the calculated MR also confirms the real MIT happened at $\sim 230\ \text{K}$ because the transition temperature will gradually increase with increase in the magnetic fields. Although the sharp peak in the ρ - T of LHMO(0.3) is not obvious (Fig. 1(c)), the $d\rho/dT$ curve presents a significant

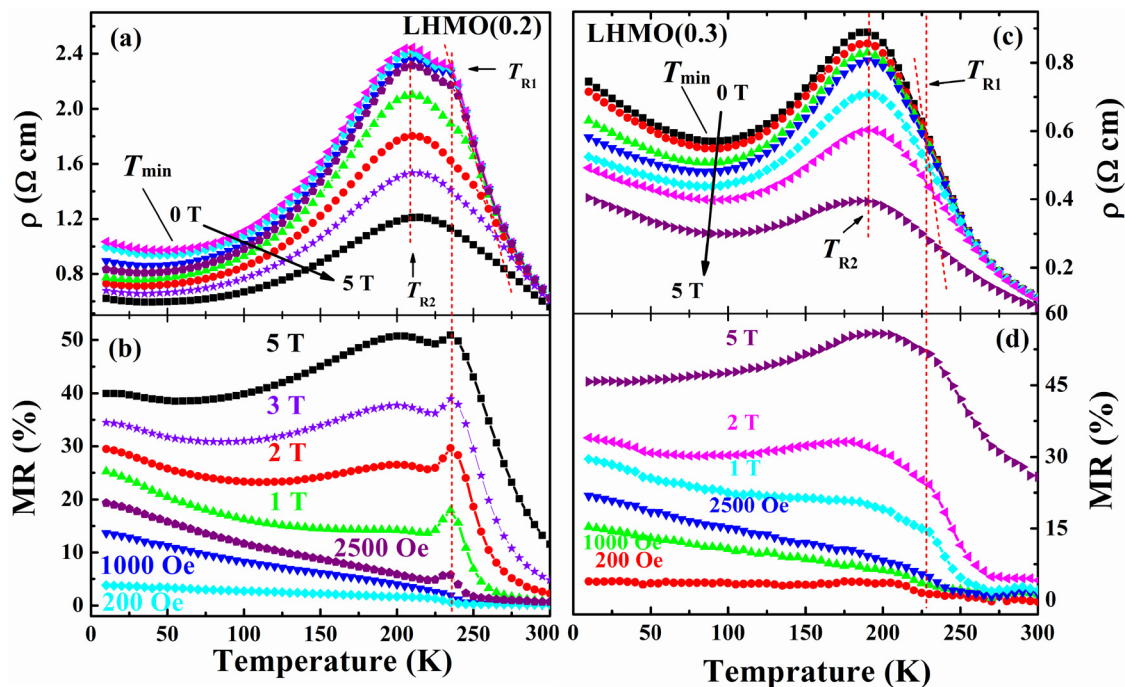


FIG. 1. The temperature dependence of resistivity (ρ) [(a) and (c)] and MR [(b) and (d)] for LHMO(0.2) and LHMO(0.3) under various magnetic fields, respectively. The arrows in the figures point out the positions of the resistivity minimum. The dashed lines in the figures are guidelines for eyes.

difference at the temperature of sharp peak (~ 220 K) and broad peak (~ 190 K). Many previous works gave evidences that the presence of grains and GB modifies the transport property in ceramic manganites as compared to single crystal and thin film samples. Unlike the sharp drop observed near the MIT temperature in the epitaxial thin films, the resistivity of a polycrystalline samples exhibits a wide maximum resistivity at a temperature below T_c . Such a shoulder-like feature had also been observed for oxygenated $\text{La}_{2/3}\text{Ba}_{1/3}\text{MnO}_3$ and $\text{La}_{0.7}\text{Ce}_{0.3}\text{MnO}_3$ samples.^{15,16} The MR in the polycrystalline and single crystal samples also show a great difference. In the single crystal thin films, there is a colossal MR in the vicinity of T_c and a very small MR apart from it. On the other hand, the polycrystalline samples have an appreciable MR at all temperature regions, which usually manifests a large MR even at the low temperature region. As shown in Figs. 1(b) and 1(d), the MRs of LHMO(0.2) and LHMO(0.3) are 40% and 45.3% measured at 5 K under magnetic field of 5 T, respectively. These values are much larger than the MR observed in the other single crystal films under the same conditions. It is noteworthy that there is a resistivity upturn which appears at low temperature. The resistivity minimum T_{\min} is 41.6 and 92.9 K for LHMO(0.2) and LHMO(0.3), respectively. The result is similar to that obtained on the other hole-doped ceramic manganites.²⁵ They also point out that it cannot be attributed to the charge-orbital ordering effects due to the weak upturn of resistivity.

We further investigate the resistivity minimum behavior under different applied magnetic fields from 0 to 5 T at low temperature. As shown in Fig. 2(a), the scatters represent the experimental results measured in the temperature range of 5–100 K. The resistivity minimum behavior of LHMO(0.2)

is strongly dependent on the magnetic fields, which makes it quite different from the Kondo effect. The significant change is that T_{\min} shifts first to the lower temperature as the magnetic fields increasing to 0.5 T, and then moves back to the higher temperature when the magnetic fields further increase to 5 T. The same variation trend of T_{\min} is found on the LHMO(0.3) sample, as shown in the scatters of Fig. 2(b). The difference between the LHMO(0.3) and LHMO(0.2) is that the turning point of T_{\min} for LHMO(0.3) is at magnetic field of 0.75 T. The field dependence of T_{\min} for LHMO(0.2) and LHMO(0.3) is shown in Fig. 3. Our results are quite different from previous works, no matter the T_{\min} moves monotonously toward lower (or higher) temperature with the increase of applied fields and upturn disappears at a certain field as in Refs. 8 and 13, or the T_{\min} moves first to the higher temperature at low fields and then to lower temperature as magnetic fields further increase (as in Ref. 9). In order to give a clear view of the effects of applied magnetic fields to the resistivity upturn, we normalized the resistivity to that of 100 and 150 K for LHMO(0.2) and LHMO(0.3), as shown in Figs. 4(a) and 4(b), respectively. It is obvious to find that the resistivity upturn below T_{\min} is rapidly suppressed at low magnetic fields (present as black hollow symbols). However, this resistivity upturn behavior becomes intense as magnetic fields increasing over 0.75 T (present as red solid symbols), neither saturated nor disappeared as described by previous works. We introduced the expression of depth of resistivity minimum $\Delta\rho$ in order to represent the degree of upturn behavior at low temperatures, which can be written as

$$\Delta\rho = \frac{\rho_{5\text{K}} - \rho_{T_{\min}}}{\rho_{T_{\min}}}, \quad (1)$$

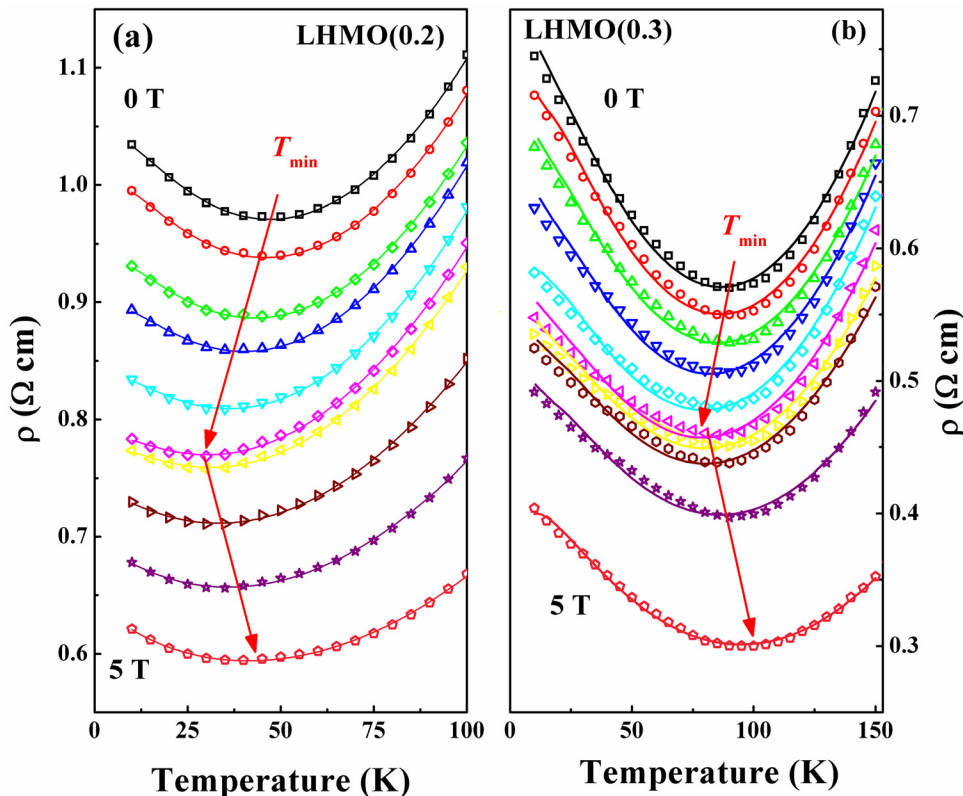


FIG. 2. The expanded view of resistivity as a function of temperature under magnetic fields from 0 to 5 T for (a) LHMO(0.2) and (b) LHMO(0.3). The scatters in the figures represent the experimental results. The solid lines are the fitted curves using Eq. (8). The arrowed lines point out the variation trends of the temperatures at resistivity minimum T_{\min} .

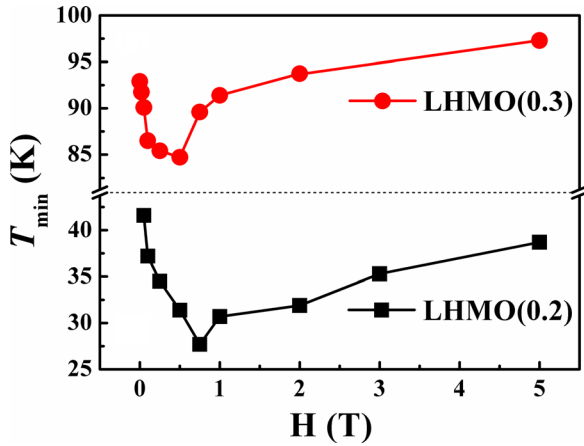


FIG. 3. (The magnetic field dependence of the temperatures at resistivity minimum T_{\min} for LHMO(0.2) (below) and LHMO(0.3) (upper).

where, ρ_{5K} and $\rho_{T_{\min}}$ represent the resistivity measured at 5 K and T_{\min} , respectively. Figure 5 shows the $\Delta\rho$ as a function of applied magnetic fields. The $\Delta\rho$ of LHMO(0.2) and LHMO(0.3) samples present a rapid decrease in the range of low applied field, $H < 0.75$ T, and an increase almost linearly

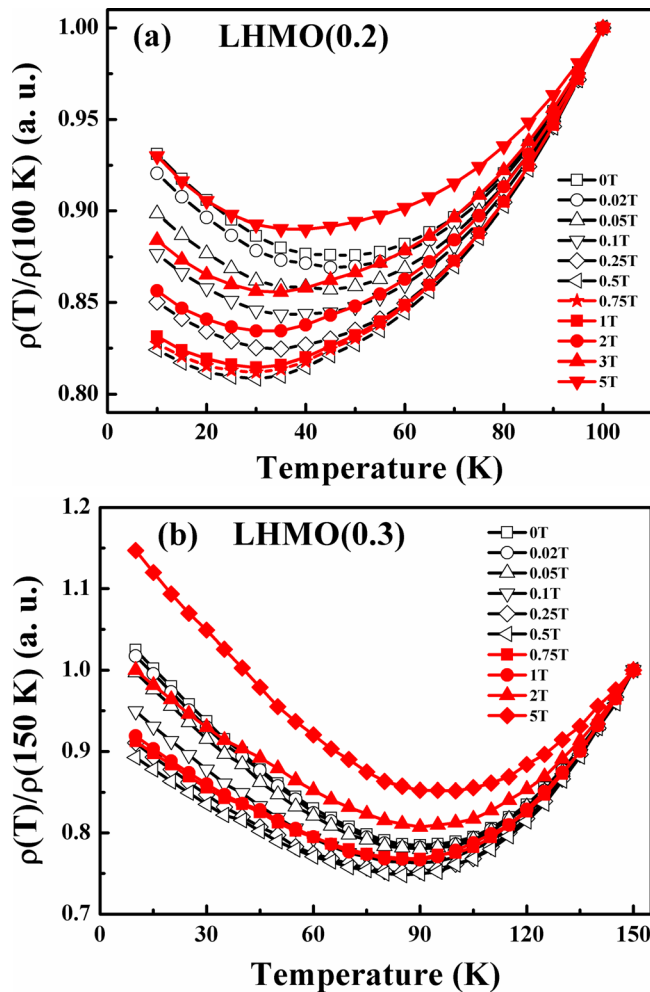


FIG. 4. The normalized resistivity as a function of temperature under magnetic fields from 0 to 5 T for (a) LHMO(0.2) and (b) LHMO(0.3). The hollow symbols and solid symbols present the normalized resistivity at low magnetic fields region and high magnetic fields region, respectively.

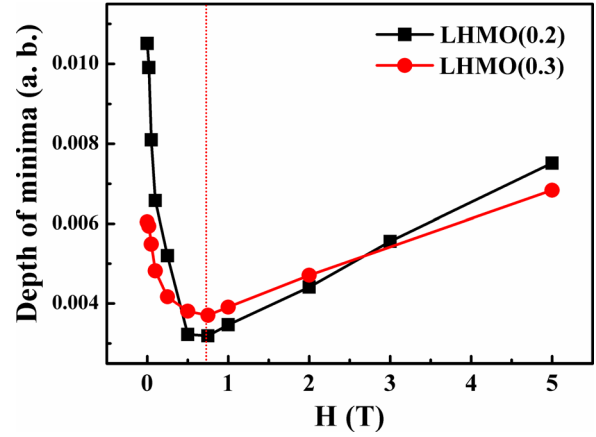


FIG. 5. The depth of minimums, which calculated from Eq. (1), as a function of applied magnetic fields for LHMO(0.2) and LHMO(0.3). The dashed line shows the possible boundary of low and high magnetic field regions.

when magnetic fields above 0.75 T. The slopes of $\Delta\rho$ -H curves in two different regions indicate that the low-temperature resistivity is more sensitive to the magnetic field at low field region.

In order to understand the origin of the observed resistivity minimum, several different models are taken into account, including spin dependent scattering, QCC effects, and so on. Based on the results of low-temperature resistivity is sensitive to the magnetic fields, we first consider that the resistivity minimum partly originate from spin dependent scattering which is proven to be suppressed by external magnetic fields and is also the general characteristic of polycrystalline samples. The resistivity of system under the model of spin dependent scattering can be described as follows:

$$\rho(T, H) = \rho_0 + \rho_s(T, H) \ln T, \quad (2)$$

where ρ_0 is the residual resistivity and $\rho_s(T, H)$ is the spin dependent scattering resistivity. However, when we tried to fit the results obtained from experiments simply by Eq. (2), it has distinct departure for all the scatters measured at low temperature. It may not be suitable to consider the single factor of spin dependent scattering affecting our observed behavior. It is well known that the low-temperature resistivity will be significantly affected by the QCC effects for an intrinsically disordered system. The QCC effect originated from the weak localization and e - e interaction.²⁷ The total resistivity of the system in the first-order correction can be given by the following expression:

$$\rho(T, H) = \rho_0 + \rho_m(T, H) - \rho_0^2 [\sigma_{ee}(T, H) + \sigma_{wl}(T, H)], \quad (3)$$

where the $\rho_m(T, H)$ is the magnetic resistivity contributed from the anisotropic MR and magnon scattering, $\sigma_{ee}(T, H)$ and $\sigma_{wl}(T, H)$ are the conductivities due to the e - e interaction and the weak localization, respectively. In our case, the magnetic fields are applied perpendicular to the samples. Thus, $\rho_m(T, H)$ can be seen as a constant changing with

temperature but provides no contribution as magnetic field changing. Generally, the $\sigma_{wl}(T, H)$ can be also neglected for two reasons. On the one hand, the weak localization results from the interference of complementary electron waves, which are already destroyed by the strong spontaneous ferromagnetic fields far below T_c . On the other hand, the weak localization effect only plays a key role in affecting the physical properties of manganites when the film thickness is very thin. As reported by Maritato *et al.*, the weak localization effect becomes effective when film thickness below 20 nm.¹² For our LHMO polycrystalline bulk samples, the effect of weak localization is inconsiderable under the applied magnetic fields. Therefore, the e - e interaction will dominate in the QCC effect.

At low temperatures, the resistivity can be described by considering the elastic scattering part $\rho_{el}(T, H)$ (including Coulomb interaction and electron-impurities) and inelastic scattering part (including electron-phonon interaction, electron-magnon interaction, etc.) $\rho_{in}(T, H)$,

$$\rho(T, H) = \rho_{el}(T, H) + \rho_{in}(T, H). \quad (4)$$

According to the previous works,^{8-10,12-14,28} the elastic resistivity due to the quantum correction, combining with the effects of e - e interaction and disorder, can be written as Eq. (5). At the same time, the resistivity due to the inelastic scattering can be written as Eq. (6),

$$\rho_{el}(T, H) = -\rho_e T^{1/2}, \quad (5)$$

$$\rho_{in}(T, H) = \rho_p T^p, \quad (6)$$

where the ρ_e and ρ_p are the e - e interaction coefficient and the e - p interaction coefficient, respectively. We substitute Eqs. (5) and (6) into Eq. (4). Meanwhile, we ignore the $\rho_m(T, H)$ and $\sigma_{wl}(T, H)$ sections when considering Eq. (3). Therefore, the total resistivity originated from QCC effect can be obtained as

$$\rho(T, H) = \rho_0 - \rho_e T^{1/2} + \rho_p T^p. \quad (7)$$

Usually, p is equal to 2 as reported in the previous works.⁸ We try to fit the experiment resistivity under different magnetic fields with Eq. (7). Again, we could not get well-fitted curves no matter in the lower magnetic fields or higher magnetic fields. Therefore, we have to consider combining two possible mechanisms together. Thus, the total resistivity of system can be obtained as

$$\rho(T, H) = \rho_0 - \rho_e T^{1/2} + \rho_s \ln T + \rho_p T^2. \quad (8)$$

We fit the experiment resistivity under all the magnetic fields to Eq. (8). The fitted results are present with the color solid lines in Fig. 2. It can be found that all the data can be well fitted considering both terms of $\ln T$ and $T^{1/2}$. The good agreement between experiment data and fitted curves also confirm our assumption of the resistivity upturn behavior, which may come from both spin dependent scattering model and QCC effect model (e - e interaction and disorder). Xu *et al.* also declared that both e - e interaction and spin dependent scattering should be taken into account in the low-temperature upturn behavior of the polycrystalline $\text{La}_{2/3}\text{Ca}_{1/3}\text{MnO}_3$ samples at the low magnetic fields ($H < 1$ T). However, they found that the experiment results obtained in the higher fields could be fitted well without accounting the spin dependent scattering in terms of $\ln T$, which is the little difference between their work and ours.

The corresponding coefficients (ρ_0 , ρ_s , ρ_e , and ρ_p) are shown in Table I. Although the fittings are only the results of the phenomenological analysis, all the values of corresponding coefficients cannot reflect the real nature of underlying physics. As shown in Table I, we can find that all the coefficients decrease as magnetic fields increasing. For the residual resistivity, ρ_0 , a slightly decrease is found with an increase of magnetic field. It exhibits a usual behavior compared with a good conductor, which should not depend on the magnetic fields. Nevertheless, this variation trend of ρ_0 is coincidence

TABLE I. The fitting results of the coefficients in Eq. (8) for all the magnetic fields changing from 0 to 5 T. The separated row in the middle of the table shows the different results for LHMO(0.2) and LHMO(0.3), respectively.

$\rho(H, T) = \rho_0 - \rho_e T^{1/2} + \rho_s \ln T + \rho_p T^2$								
	LHMO (0.2)				LHMO (0.3)			
H(T)	ρ_0 (Ω cm)	ρ_e ($10^{-2} \Omega$ cm $\text{K}^{-1/2}$)	ρ_s ($10^{-2} \Omega$ cm (lnK) $^{-1}$)	ρ_p ($10^{-5} \Omega$ cm K^{-2})	ρ_0 (Ω cm)	ρ_e ($10^{-1} \Omega$ cm $\text{K}^{-1/2}$)	ρ_s ($10^{-1} \Omega$ cm (lnK) $^{-1}$)	ρ_p ($10^{-5} \Omega$ cm K^{-2})
0	1.06	8.29	10.12	4.12	0.626	1.54	2.57	3.06
0.02	1.01	7.94	9.85	4.04	0.595	1.50	2.52	2.98
0.05	0.95	7.05	8.81	3.87	0.558	1.40	2.38	2.80
0.1	0.90	6.48	8.21	3.82	0.507	1.32	2.30	2.74
0.25	0.85	5.33	6.57	3.62	0.458	1.23	2.16	2.62
0.5	0.79	3.86	4.65	3.25	0.417	1.17	2.12	2.49
0.75	0.78	3.82	4.57	3.14	0.413	1.09	1.97	2.25
1	0.78	3.61	4.25	3.11	0.411	1.06	1.89	2.21
2	0.75	3.09	3.07	2.64	0.402	0.92	1.61	1.78
3	0.71	2.44	1.81	2.14	N/A	N/A	N/A	N/A
5	0.66	2.08	1.04	1.66	0.357	0.74	1.19	1.34

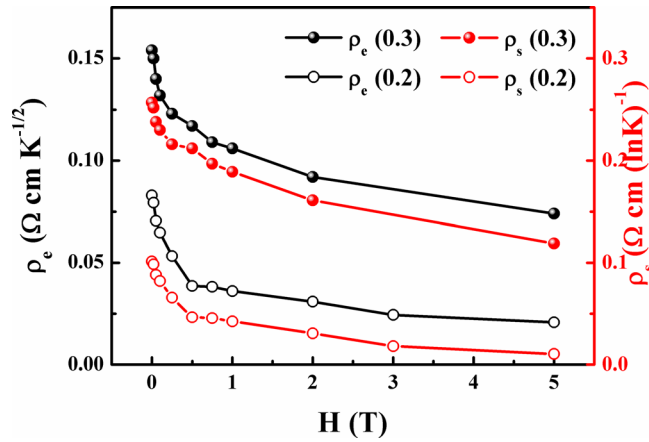


FIG. 6. The best fitted coefficients of ρ_e and ρ_s , which obtained are from Eq. (8), as a function of applied magnetic fields for LHM0(0.2) and LHM0(0.3).

with the results found in Refs. 9, 10, and 12. The electron-phonon resistivity ρ_p is found much smaller than the other coefficients by over three orders, indicating the weak influence to the total resistivity. Thus, the main factors affect the total resistivity under various magnetic fields are ρ_s and ρ_e . Fig. 6 shows the ρ_s and ρ_e change as a function of magnetic fields. The ρ_s and ρ_e show the same variation trend as T_{\min} and were found decreasing with the increase of magnetic fields. There is an obvious boundary between the low magnetic field region ($H < 0.75$ T) and high magnetic field region ($H > 0.75$ T). In the lower field region, both ρ_s and ρ_e show a rapid drop as increasing the magnetic fields until $H = 0.75$ T, while these variations become moderate when magnetic field larger than 0.75 T. We think that the resistivity minimum behavior at low-temperature comes from the competition of two main contributions: one increase, another decrease as magnetic fields increasing. An applied magnetic field can align the spins of the magnetic domains to the direction of fields and induce the deconfinement of the motion of the spin-polarized carriers. Then, the tunneling of conduction electrons between the antiferromagnetically coupled grains will happen due to the reduced GB's barrier. However, this tunneling through GB is strongly decreased as magnetic field increasing. Therefore, we believe that strong resistivity dependence of fields on low magnetic fields may be attributed to the domination of spin dependent scattering (GB tunneling). As the magnetic fields increasing above 0.75 T, the effect of spin dependent scattering decrease and $e-e$ interaction will play a key role in dominating the low-temperature resistivity minimum behavior due to its weak dependence on the magnetic fields.

Furthermore, we also confirm the effect of disorder to the resistivity upturn behavior in this system. As we know that, the $e-e$ interaction will be enhanced by the magnetic disorder degree in the system. Jia *et al.*¹³ studied the effects of the local lattice distortion induced disorders to the resistivity upturn behavior. They introduced the *in situ* tunable ferroelectric-poling-induced in-plane strain to the manganite thin films in order to investigate the influence to the QCC effect. It was found that the resistivity upturn and T_{\min} are significantly suppressed after ferroelectric poling due to the reductions of lattice distortion of MnO_6 octahedral and

orbital disorders. However, another kind of disorder could be the random potential fluctuations due to the different doping size of ions and doping levels. In our case, two different doping levels ($x = 0.2$ and 0.3) of LHM0 compounds were studied. From Figs. 2 and 3, we can find that, comparing with the results on the LHM0(0.2), the resistivity upturn behavior of LHM0(0.3) grows much more tempestuous and T_{\min} is nearly twice larger than that of LHM0(0.2). As shown in Fig. 6, the ρ_0 of LHM0(0.3) is smaller than that of LHM0(0.2) the reason of that probably is the higher doping level induced more carriers in the compounds. However, ρ_s and ρ_e of LHM0(0.3) are larger than those of LHM0(0.2). The higher doping level will induce higher disorder degree in the system, including the doped carriers' density and the impurity secondary phase reported in our previous work.²⁴ Thus, it is understandable that the observed resistivity upturn becomes aggravated and the T_{\min} moves to the higher temperature. These results indicate that the $e-e$ interaction enhanced by disorder may play an important role in determining the low-temperature resistivity minimum behavior of LHM0 compounds. The effect of different doping levels on the resistivity upturn gives a direct evidence of the presence of QCC effect in LHM0 at low-temperature. At the same time, another impact factor, which is the magnetic disorder and frustration in the FM ground state, should also be taken into account in our case. As reported by Muthuselvam *et al.*,²⁵ this low-temperature minima appears due to the competition between the weak FM grain boundaries and strong FM grains. The higher Hf doping level will introduce more secondary phases, which is magnetically, and meanwhile the magnetic disorder and grain boundaries will increase correspondingly. That maybe one of the reasons that the T_{\min} of LHM0(0.3) is higher than that of LHM0(0.2). The same result was also found in other magnetic oxides by increasing the doping level of nonmagnetic elements.²⁶ Our results may be different from the explanation on the polycrystalline $\text{La}_{0.5}\text{Pb}_{0.5}\text{MnO}_3$ compounds in Ref. 8. They attributed the single factor model of spin-polarized intergrain tunneling to understand low-temperature resistivity minimum behavior. In our case, we think both models of spin dependent scattering and $e-e$ interaction should take into consideration in order to fully understand the low-temperature resistivity minimum in these electron-doped LHM0 manganites.

IV. CONCLUSIONS

In summary, the low-temperature resistivity minimum behavior and its dependence on the magnetic fields are systematically studied on the polycrystalline LHM0 compounds with two different doping levels $x = 0.2$ and 0.3 . The results show that the temperature at resistivity minima T_{\min} shifts first to the lower temperature at low magnetic fields $H < 0.75$ T, then moves back to the higher temperature as magnetic fields increasing above 0.75 T. The experiment results were fitted by considering both terms of $\ln T$ and $T^{1/2}$, indicating the observed phenomenon in LHM0 can be understood taking into account both spin dependent scattering and $e-e$ interaction. The effect of different doping levels to the resistivity upturn also gives a direct evidence of the

presence of e - e interaction in LHMO at low-temperature. At low magnetic field region, spin dependent scattering model dominates the low-temperature resistivity minimum behavior, while the e - e interaction plays a key role at the high magnetic field region. Our results verify that e - e interaction is a general characteristic in the strong correlated manganites. Furthermore, we also want to note that it is the first time to observe such low-temperature resistivity behavior in the tetravalent Hf-doped manganites. To fully understand this behavior in LHMO, many more experiments on the single crystal thin films and theoretical calculations are needed.

ACKNOWLEDGMENTS

This work was supported by a grant of the Research Grant Council of Hong Kong (Project No. HKU702409P), the URC of the University of Hong Kong, and also granted by the National Natural Science Foundation of China and the National Basic Research Program of China.

- ¹J. Fontcuberta, B. Martinez, A. Seffar, S. Pinol, J. L. GarciaMunoz, and X. Obradors, *Phys. Rev. Lett.* **76**, 1122–1125 (1996).
- ²C. H. Booth, F. Bridges, G. H. Kwei, J. M. Lawrence, A. L. Cornelius, and J. J. Neumeier, *Phys. Rev. Lett.* **80**, 853–856 (1998).
- ³A. Urshibara, Y. Moritomo, T. Arima, A. Asamitsu, G. Kido, and Y. Tokura, *Phys. Rev. B* **51**, 14103 (1995).
- ⁴A. P. Ramirez, P. Schiffer, S.-W. Cheong, C. H. Chen, W. Bao, T. T. M. Palstra, P. L. Gammel, D. J. Bishop, and B. Zegarski, *Phys. Rev. Lett.* **76**, 3188–3191 (1996).
- ⁵B. B. Van Aken, T. T. M. Palstra, A. Filippetti, and N. A. Spaldin, *Nature Mater.* **3**, 164–170 (2004).
- ⁶J. B. Philipp, L. Alff, A. Marx, and R. Gross, *Phys. Rev. B* **66**, 224417 (2002).
- ⁷E. Dagotto, *New J. Phys.* **7**, 67 (2005).
- ⁸E. Rozenberg, M. Auslender, I. Felner, and G. Gorodetsky, *J. Appl. Phys.* **88**, 2578 (2000).

- ⁹Y. Xu, J. Zhang, G. Cao, C. Jing, and S. Cao, *Phys. Rev. B* **73**, 224410 (2006).
- ¹⁰D. Kumar, J. Sankar, J. Narayan, R. K. Singh, and A. K. Majumdar, *Phys. Rev. B* **65**, 094407 (2002).
- ¹¹S. K. Singh, S. B. Palmer, D. M. Paul, and M. R. Lees, *Appl. Phys. Lett.* **69**, 263 (1996).
- ¹²L. Maritato, C. Adamo, C. Barone, G. M. De Luca, A. Galdi, P. Orgiani, and A. Yu. Petrov, *Phys. Rev. B* **73**, 094456 (2006).
- ¹³R. R. Jia, J. C. Zhang, R. K. Zheng, D. M. Deng, H.-U. Habermeier, H. L. W. Chan, H. S. Luo, and S. X. Cao, *Phys. Rev. B* **82**, 104418 (2010).
- ¹⁴S. Mukhopadhyay and I. Das, *Europhys. Lett.* **79**, 67002 (2007).
- ¹⁵H. L. Ju, J. Gopalakrishnan, J. L. Peng, Qi. Li, G. C. Xiong, T. Venkatesan, and R. L. Greene, *Phys. Rev. B* **51**, 6143 (1995).
- ¹⁶S. Das and P. Mandal, *Ind. J. Phys.* **71**, 231 (1997); S. Das and P. Mandal, *Z. Phys. B: Condens. Matter* **7**, 104 (1997); P. Mandal and S. Das, *Phys. Rev. B* **56**, 15073 (1997).
- ¹⁷J. R. Gebhardt, S. Roy, and N. Ali, *J. Appl. Phys.* **85**, 5390–5392 (1999).
- ¹⁸C. Mitra, P. Raychaudhuri, J. John, S. K. Dhar, A. K. Nigam, and R. Pinto, *J. Appl. Phys.* **89**, 524–530 (2001).
- ¹⁹H. Chou, C. B. Wu, S. G. Hsu, and C. Y. Wu, *Phys. Rev. B* **74**, 174405 (2006).
- ²⁰P. Raychaudhuri, C. Mitra, P. D. A. Mann, and S. Wirth, *J. Appl. Phys.* **93**, 8328–8330 (2003).
- ²¹G. T. Tan, S. Dai, P. Duan, Y. L. Zhou, H. B. Lu, and Z. H. Chen, *Phys. Rev. B* **68**, 014426 (2003); G. T. Tan, S. Y. Dai, P. Duan, Y. L. Zhou, H. B. Lu, and Z. H. Chen, *J. Appl. Phys.* **93**, 5480–5483 (2003); G. T. Tan, P. Duan, G. Yang, S. Y. Dai, C. B. Lin, Y. L. Zhou, H. B. Lu, and Z. H. Chen, *J. Phys.: Condens. Matter* **16**, 1447 (2004).
- ²²J. Gao, S. Y. Dai, and T. K. Li, *Phys. Rev. B* **67**, 153403 (2003).
- ²³L. Wang and J. Gao, *J. Appl. Phys.* **103**, 07F702 (2008).
- ²⁴E. J. Guo, L. Wang, Z. P. Wu, L. Wang, H. B. Lu, K. J. Jin, and J. Gao, *J. Appl. Phys.* **110**, 113914 (2011).
- ²⁵I. P. Muthuselvam and R. N. Bhowmik, *J. Alloys Compd.* **511**, 22–30 (2012).
- ²⁶A. Poddar, R. N. Bhowmik, and I. Panneer Muthuselvam, *J. Appl. Phys.* **108**, 103908 (2010).
- ²⁷M. Ziese, *Phys. Rev. B* **68**, 132411 (2003).
- ²⁸B. L. Altshuler and A. G. Aronov, *Sov. Phys. JETP* **50**, 968 (1979).